ANALYSIS OF LAMINAR PREMIXED COMBUSTION FLAME CHARACTERISTICS FOR SHALE GAS, BIOMASS GAS, AND COALBED GAS

Guoyan CHEN [*], Wenhao ZHANG[1], Anchao ZHANG[1], Haoxin DENG[1], Xiaoping WEN[1], Bo YANG[1], Hongliang ZHOU[1]

[*1] School of Mechanical and Power Engineering, Henan Polytechnic University, Jiaozuo 454003, China

[*] 254568182@qq.com

In this paper, three clean gases (shale gas, biomass gas, and coalbed gas) are simulated by using Chemkin-Pro software. The GRI 3.0 mechanism, which exhibits superior predictive performance overall, is chosen for numerical simulation based on comparative analysis. The comprehensive analysis of the effects of fuel components on flame speed and temperature in the three mixtures. Based on the laminar burning velocity, the numerical decoupling method is used to separate the chemical and physical effects of CH_4, as well as the dilution, thermal, and chemical effects of CO_2. At the same time, verification and analysis are carried out by sensitivity analysis and flame structure analysis. Sensitivity analysis is employed to evaluate the impact of key fundamental reactions on laminar burning velocity and temperature, while flame structure analysis is utilized to ascertain variations in crucial species and temperatures during flame combustion.

Key words*: Laminar burning velocity; Equivalent ratio; Sensitivity; Adiabatic flame temperature*

1. Introduction

Non-conventional energy such as shale gas, biomass gas, and coalbed gas are mentioned more and more frequently. With the demand for clean energy in society today, this kind of energy is increasingly valued. As an unconventional natural gas, shale gas [1-3] is beneficial in meeting the huge demand for clean energy for economic development and controlling pollutant emissions. As a renewable energy, biomass gas [4-6] can replace fossil fuels to a certain extent and reduce the output of pollutants. Coalbed gas [7-9] is also one the unconventional natural gas, which can be mixed with natural gas, and it produces almost no waste gas after combustion.

To make effective use of these gases for better practical use, a more complete understanding of their combustion characteristics is necessary. Cardona Vargas et al. [10] analyzed the combustion characteristics of different shale gas mixtures by numerical and experimental methods, including adiabatic flame temperature and calorific value, and obtained the most important element reaction and the influence of dilution gas. Ozturk [11] computationally investigated the adiabatic and partial premixed combustion of several shale gases at different flow rates, inlet temperatures, equivalence ratios, and pressures. In terms of biomass gas, Bhasker [12] from India studied the combustion characteristics of biomass gas and found that reducing the percentage of CO_2 in the fuel increased the combustion rate, thermal efficiency, and power of the engine. Research on coalbed gas, the laminar flame of the CH_4/N_2/air mixture was studied by Miao et al. [13] using a constant volume combustion

bomb and a high-speed ripple shadow system. Considering the nonlinear effect of tension, the experimental data were analyzed by conventional and nonlinear methods. Compared with the results, different methods have little effect on flame velocity, but a significant effect on Markstein length. Zheng et al. [14] investigated the turbulent and laminar combustion characteristics of coalbed gas/air-premixed flames in a constant volume combustion bomb. The findings indicate that the tension-free flame velocity of mixed gas premixed flame decreases with increasing N_2 volume fraction and pressure. The Markstein length increments with augmented N_2 volume fraction and equivalence ratio and decreases with augmented initial pressure.

Shale gas, biomass gas, and coalbed gas are all unconventional natural gases, containing CH_4 as a primary component, especially in shale gas and coalbed gas, while the CH_4 content in biomass gas varies depending on the gasification process. Analysis of many scholars' previous research indicates that studies have typically focused on the analysis of single gases, with limited comparative analysis involving multiple gases. Therefore, a comprehensive analysis of the laminar combustion of these three gases is helpful for studying the impact of varying combustible component concentrations in gases. Based on the laminar burning velocity (S_L), the physical and chemical effects of CH_4 have been separated using the numerical decoupling method, as well as the dilution, thermal, and chemical effects of CO_2. While there has been analytical research on the physical effects of diluents, studies on chemical effects are relatively scarce. Additionally, the decoupling analysis of combustible gases contributes to a deeper understanding of S_L.

The study of premixed laminar flow combustion is relatively more basic. Meanwhile, the S_L is an important index to test the chemical reaction mechanism of fuel and a key parameter to calculate the diffusion of turbulent premixed flame [15-17]. Studying the basic combustion characteristics of fuel is the only way to understand the fuel combustion process, improve efficiency and develop clean energy. Therefore, the combustion research of premixed laminar flow is of great significance [18-20].

2. Numerical simulation

According to information that the fuel composition of the gas mixture is very complex, the instability of flame propagation [21,22] and the inevitable error of the experiment [23] itself are great challenges for the flame analysis of the gas mixture under laboratory conditions. Therefore, the effects of different fuel components and experimental conditions on chemical reaction rate can be analyzed in detail by numerical simulation method, component formation rate [24] or consumption rate, flame temperature change, and so on from the perspective of chemical dynamics.

Tab. 1 Chemical kinetics model

Mechanisms	No. of species	No. of reactions	Reference
GRI-3.0	53	325	[25]
USC	110	784	[26]
San Diego	58	270	[27]

The laminar combustion of fuel is simulated in this study using the pre-mixed components in the Chemkin-Pro software, under normal temperature and pressure (T_0 = 300 K, P_0 = 0.1 MPa) conditions [28]. For each simulation condition, the adaptive heavy grid method is employed with a convergence criterion set at CURV and GRAD values of 0.02, while limiting the maximum number of grids to 900 [29]. Tab. 1 includes GRI-3.0, USC-II ,and San Diego. All these models have been

extensively validated, including pressure, temperature, etc. The above mechanism papers have been used in many articles [30-33].

Tab. 2 Gas fuel components

Shale gas	Fuel mixture (vol %)			**Biomass gas**	Fuel mixture (vol %)					**Coalbed gas**	Fuel mixture (vol %)		
	X_{CH4}	X_{C2H6}	X_{C3H8}		X_{CH4}	X_{H2}	X_{CO}	X_{CO2}	X_{N2}		X_{CH4}	X_{N2}	X_{CO2}
αBasics	70	20	10	αBasics	10	30	30	25	5	αBasics	70	20	10
αCH_4-0.1	10	80	10	αCH_4-0.3	30	30	30	5	5	αCH_4-0.1	10	50	40
αCH_4-0.5	50	40	10	αCH_4-0.4	40	30	30	0	0	αCH_4-0.4	40	50	10
αCH_4-0.8	80	10	10	αCH_4-0.6	60	30	10	0	0	αCH_4-0.9	90	0	10
αCH_4-0.9	90	0	10	αCH_4-0.9	90	10	0	0	0	-	-	-	-

Tab. 2 respectively shows the fuel components of shale gas [34-36], biomass gas [37-39], and coalbed gas [40-42]. This paper focuses on studying the influence of the change of fuel components on flame characteristics.

3. Results and discussion

3.1. Comparative analysis of three mechanism conditions

The experimental method used in this paper is the same as that of Zhang et al.[43], and the details of the experimental method have been elaborated in their paper. A schlieren system is added to the original experimental platform for capturing flame propagation images, and the schematic diagram of the experimental platform is shown in Fig. 1. The spherical expanding flame method measures the S_L of the mixed fuel under normal temperature and pressure(T_0 = 300 K, P_0 = 0.1 MPa) conditions.

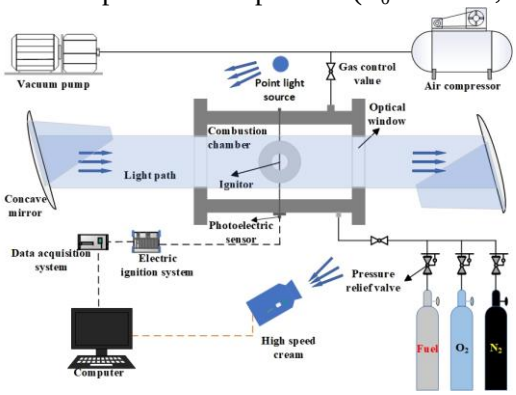

Fig. 1 Schematic diagram of the experimental platform

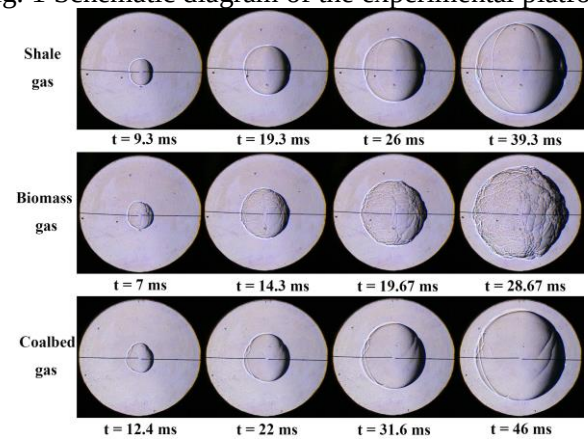

Fig. 2 Spherical expansion flame image

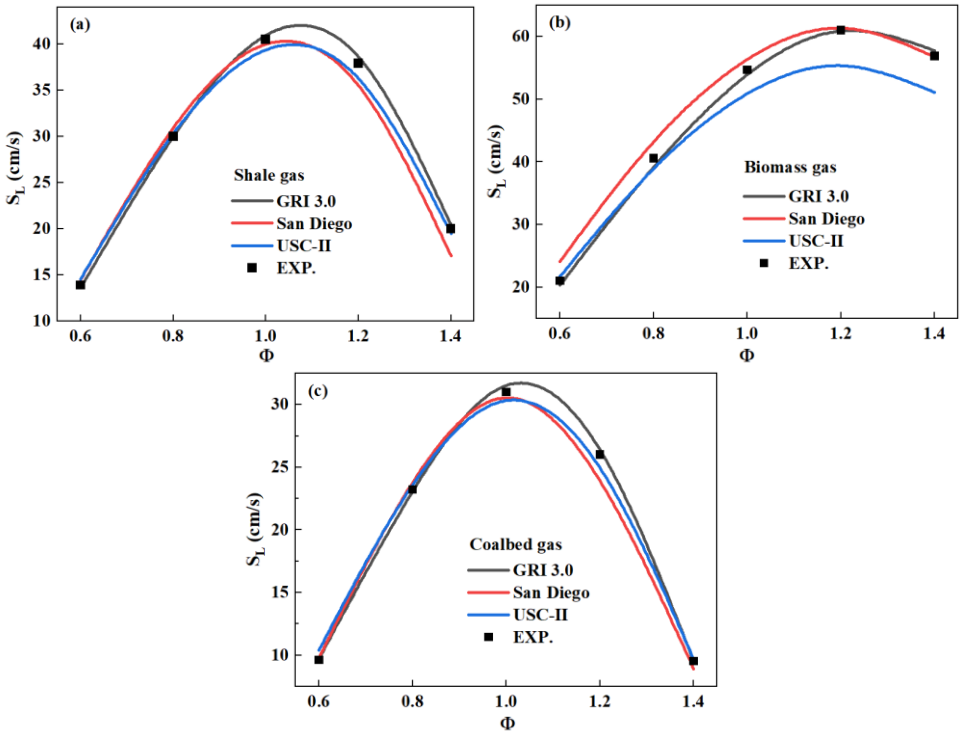

Fig. 3 Laminar burning velocity(S_L) of three gases

The basic components of three types of gas are selected for the experiment, with an equivalence ratio ranging from 0.6 to 1.4 at intervals of 0.2. The flame propagation images are shown in Fig. 2. In Fig. 3, the experimental data is compared with the predicted data from three chemical models. The S_L of the three kinds of gas mixtures increased first and then decreased. The difference is that shale gas peaks at an equivalent ratio of 1.1. Biomass gas peaks at about 1.2, and coalbed gas flame speed peaks at an equivalent ratio of 1. This paper focuses on the comparative analysis of the difference between three gas components to study the influence of the change of fuel components on the flame. Based on the comparison between experimental and simulated data in the figure, overall, the GRI 3.0 mechanism provides better predictions for the S_L of the three gases. Therefore, subsequent analysis will adopt the GRI 3.0 mechanism.

3.2. Effect of composition change on laminar burning velocity

The effects of increasing the CH_4 content in syngas on its S_L are manifold. These include chemical as well as physical effects of CH_4. The physical effect includes dilution effect and thermal effect. The chemical effect is mainly the effect of the chemical reaction of CH_4 on S_L, and the dilution effect refers to the effect of reducing the content of other combustible gases in syngas. The non-dilution physical effects usually refer to the effects of changes in thermal parameters such as specific heat and thermal diffusion coefficient, and are therefore often referred to as thermal effects.

In order to be able to decouple the analysis of physical and chemical effects on the S_L of syngas. A dummy substance FCH_4 is introduced, which has the same thermodynamic and transport mechanism as CH_4, but FCH_4 does not participate in the chemical reaction. In order to avoid the influence of the introduction of FCH_4 on the syngas equivalence ratio, FO_2 and FN_2 are introduced in the same way.

3.2.1 *Shale gas*

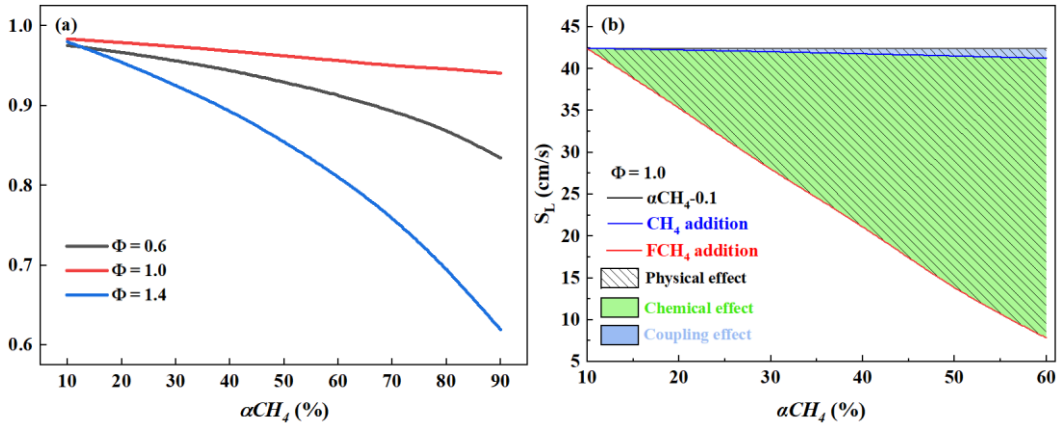

Fig. 4 The impact of CH_4 content on the laminar burning velocity of shale gas

Fig. 4(a) illustrates the ratio of S_L with different CH_4 content to the S_L without CH_4, enabling an analysis of the influence of CH_4 content on the S_L of the mixed fuel under varying equivalence ratios. The S_L diminishes with decreasing C_2H_6 concentration. At an equivalence ratio of 1, the alteration in S_L with CH_4 content is relatively insignificant, suggesting that the substitution of CH_4 for C_2H_6 has a limited influence on S_L. The second is when the equivalent ratio is 0.6, and the biggest change is when the equivalent ratio is 1.4. That is to say, in the lean fuel area, with the increase of CH_4 content, the decrease rate of S_L is lower than that in the rich fuel area.

In Fig. 4(b) a decoupling analysis is performed using the effect of FCH_4 on CH_4. The portion filled with a diagonal line indicates the physical effect of increasing CH_4 content on the S_L of shale gas. It can be observed that the physical effect of CH_4 makes the S_L of shale gas decrease almost linearly. The green-filled part is the chemical effect caused by the increase of CH_4, which promotes the increase of S_L of shale gas. The blue-filled part is the coupled effect of physical and chemical factors, i.e., overall increasing CH_4 causes a small decrease in the S_L of shale gas, which is a relatively small effect. At a CH_4 content of 20%, the ratio of the chemical effect to the physical effect of CH_4 addition is approximately 97.36%. As the CH_4 content increases, this ratio gradually decreases, reaching around 96.59% at a 60% CH_4 content. The gradual increase in the ratio of chemical effect indicates that the chemical reaction of CH_4 has a gradually increasing role in promoting the S_L of shale gas.

3.2.2 *Biomass gas*

The focus here is on the effect of CH_4 substitution of CO on the S_L of syngas. The variation of S_L of syngas with increasing CH_4 concentration (decreasing CO content) for different equivalence ratios is given in Fig. 5(a). It can be found that the S_L of syngas decreases gradually with increasing CH_4 content and the rate of decrease increases with increasing equivalence ratio.

In Fig. 5(b), a decoupling analysis is performed using the virtual substance FCH_4 to assess the independent effects of CH_4 content on the S_L of biomass gas. The region filled with diagonal lines represents the physical effect resulting from an increase in CH_4 content (from 40% to 70%), causing a reduction in the S_L of the syngas. The green-filled region signifies the chemical effect arising from the additional CH_4, as CH_4's chemical reactions promote an enhancement in S_L. The chemical effect of CH_4 addition is smaller than its physical effect. When both effects are considered together, the

addition of CH_4 leads to a decrease in the S_L of the syngas, as depicted by the blue-filled region. At a 50% CH_4 content, the ratio of the chemical effect to the physical effect is approximately 80.89%. This ratio decreases with an increase in CH_4 content, reaching around 77% at a 70% CH_4 content. This implies an increasing prominence of the physical effect, thereby restraining the S_L of the syngas.

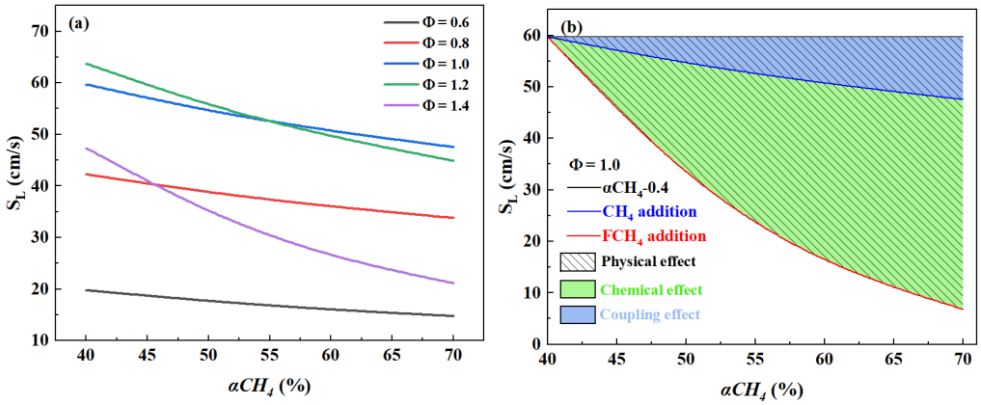

Fig. 5 Laminar burning velocity with increased CH_4 content

3.2.3 Coalbed gas

With the decrease of CO_2 and N_2 content, the change rate of S_L is different. Therefore, the S_L of CH_4/N_2, CH_4/CO_2, and $CH_4/N_2/CO_2$ is being analyzed. As can be seen in Fig. 6(a), the S_L of all three blends increased with the rise of CH_4 content, but at the same CH_4 content, the S_L of CH_4/N_2 is the highest, followed by $CH_4/N_2/CO_2$. From this, it can be judged that the carbon dioxide content of the coalbed gas S_L inhibition is more obvious.

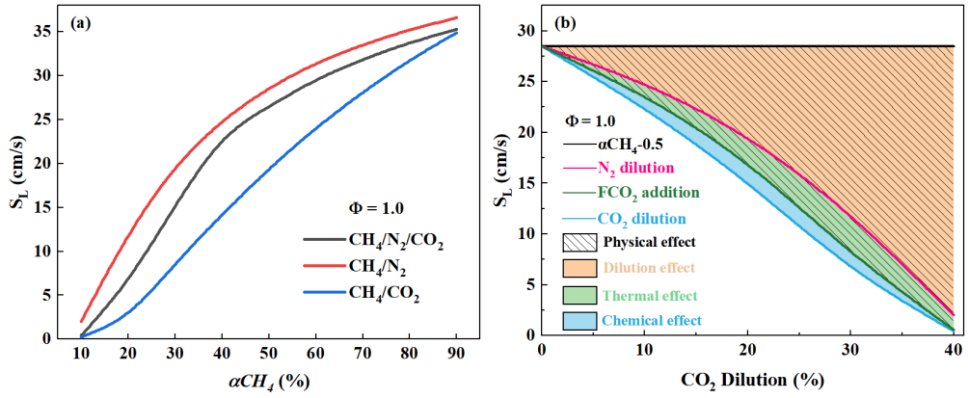

Fig. 6 The impact of N_2/CO_2 on the S_L of coalbed gas

Based on the studies of many scholars, the addition of N_2 in the mixed fuel only serves as the dilution effect [44]. Therefore, the dilution effect of adding CO_2 is determined using an equal volume fraction of N_2, as shown in Fig. 6(b). The region between FCO_2 and N_2 additions represents the thermal effect of adding CO_2 on the S_L of coalbed gas. The impact of the thermal effect diminishes after CO_2 exceeds 30%, and its proportion in relation to the physical effect decreases with increasing CO_2 concentration. As indicated by the area representing the chemical effect in the figure, the chemical effect of CO_2 inhibits the S_L of coalbed gas. The presence of both chemical and thermal effects is the reason why adding CO_2 leads to a greater reduction in the S_L of coalbed gas compared to adding an equal volume fraction of N_2.

3.3. Sensitivity analysis

To assess the significance of the fundamental response to the influence of S_L and identify the most responsive fundamental reaction to flame speed variations caused by different fuel components, a sensitivity analysis is conducted employing flow rate sensitivity coefficients [45-47]. If the sensitivity coefficient of a reaction is positive, it indicates that the reaction facilitates species formation. Conversely, if the sensitivity coefficient of a reaction is negative, it indicates that the reaction promotes species consumption.

The sensitivity coefficients of elementary reactions under normal pressure and temperature (T_0 = 300 K, P_0 = 0.1 MPa) are examined in this passage for equivalence ratios of 0.6, 1.0, and 1.4. It investigates the influence of CH_4 concentration on the primary elementary reactions of shale gas, biomass gas, and coalbed gas.

In Fig. 7(a), for shale gas, during lean combustion, chain termination reaction R99 and chain initiation reaction R38 have similar sensitivity coefficients. For the former, OH radical reacts with the CO molecule to form the H radical and stable product CO_2, while for the latter H radical decomposes the O_2 molecule to produce the O and OH radical. The whole reaction process gradually speeds up as a result of these chain reactions that can generate a lot of free radicals. The reaction R35 that consumes H radical is an important inhibition reaction. The presence of H_2O makes O_2 compete with H radical to produce the intermediate product HO_2, which reduces H group concentration and thus inhibits forward combustion.

In the case of rich combustion, chain reaction R38 becomes the most dominant forward reaction, and O_2 becomes more competitive with the H group. At the same time, chain propagation reaction R10 consumes the O group and generates the H group, increasing the concentration of the H group, thus promoting laminar burning velocity. The most significant elementary reaction at the moment to the lower H group is reaction R52, which involves CH_3 competing with the H group. There is also a large increase in the value of the sensitivity factor, indicating a more pronounced suppression of the flame speed.

The obvious changes in CH_4 content are R38, R52, R159, R119, and other reactions. As the CH_4 content increases, the consumption of O radicals produces CH_3, O radical concentration decreases, and the R38 reaction rate is accelerated. At the same time, the content of CH_3 also increased, the chain propagation reactions such as R97 and R119 also accelerated, and the sensitivity coefficient increased. At the same time, the negative sensitivity coefficient of chain reaction R52, which plays a leading role in inhibition, increased, and its inhibition of mass combustion rate increased, thus inhibiting the combustion reaction.

The chemical reactions of R38, R99, R52, and R35 in biomass gas exhibit the highest sensitivity to variations in S_L, as depicted in Fig. 7(b) and (c). During lean burning, R38 and R99 produce large amounts of OH and H radicals, which will advance the reaction rate. The reactions of R290, R166, R167, and R284 produce H groups, which increase the concentration of H groups and promote the R38 to move forward and increase the flame speed. Reactions R35, R52, and R36 that consume H groups are the main inhibition reactions. The presence of N_2 and H_2O in R35 and R36 competes with the reactions of H and O_2 to produce the intermediate product HO_2, and CH_3 in R52 competes with the reactions of H groups to produce CH_4, which generally reduces the concentration of H groups and thus inhibits the forward combustion.

In the case of rich combustion, reaction R38 is the most important positive leading reaction. Two active free radicals can be produced from each H radical (O radical and OH radical). The reaction R10 and R284 consume O radicals to generate two H radicals, thus increasing the overall H radical concentration and promoting forward combustion. The competition of CH_3 for the H group in the third body reaction R52 at this time is the most important elementary reaction that reduces the H group.

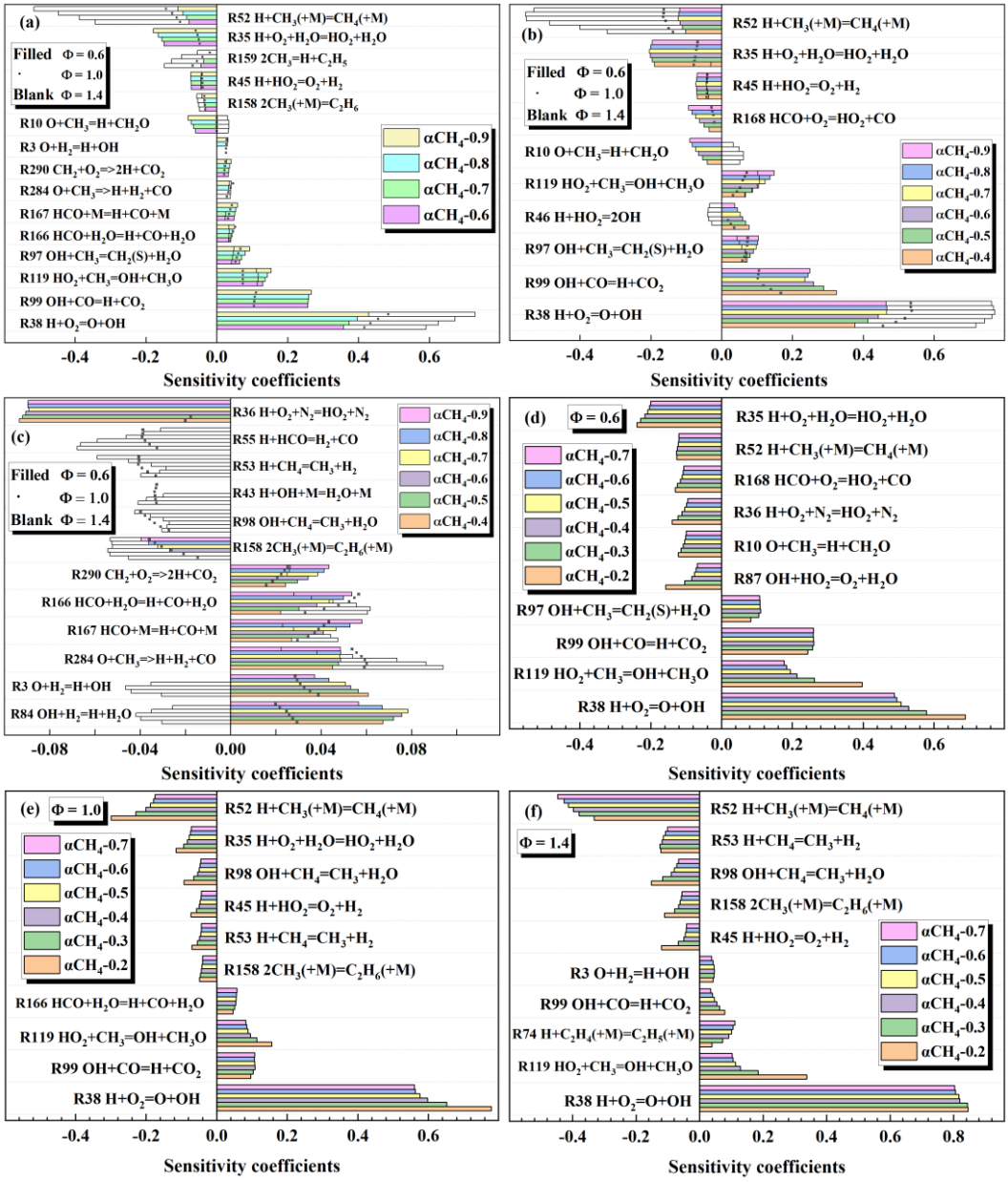

Fig. 7 Sensitivity coefficient (T_0 = 300 K, P_0 = 0.1 MPa)

According to the change of CH_4, when the proportion of CH_4 is from 0.4 to 0.7, CH_4 gradually replaces the proportion of CO content, and the positive sensitivity coefficient of R99, which is the main reaction consuming CO, gradually decreases, the catalytic effect of a chemical reaction is reduced. However, the negative sensitivity coefficients of inhibition reactions R52, R53, R55, R98, R158, etc. gradually increase, and the inhibition effect on combustion also increases. When the ratio of CH_4 content ranges from 0.7 to 0.9(CH_4 gradually replaces H_2), the sensitivity coefficient of R3 and R84 decreases, which means that the decrease of H_2 concentration makes H_2 less competitive against O and OH groups. Therefore, the sensitivity coefficient of the reaction R99, which consumes the OH

group increases slightly, and did not change much for the reaction R38. The sensitivity coefficient decreases at the time of rich combustion. The positive sensitivity coefficients of R10, R168, R98, and R158 will exhibit a decrease, while the negative sensitivity coefficients will demonstrate an increase. Consequently, this phenomenon is expected to exert a certain influence on the combustion reaction.

For coalbed gas, as depicted in Fig. 7(d), (e), and (f), it's noticeable that with changes in equivalence ratio, the primary impacting elementary reactions aren't entirely consistent. At an equivalence ratio of 0.6, the most influential forward-promoting reactions are R38, followed by R119, R99, and R97, displaying substantial promoting tendencies. The primary inhibiting reaction at this point is R35, followed by the chain termination reaction R52. As CH_4 content increases, it's observed that the concentrations of intermediate products also increase, consequently reducing the sensitivity coefficients of R38 and R119. Similarly, the absolute values of sensitivity coefficients for inhibiting reactions such as R35, R52, R168, R36, R10, and R87 also decrease with increasing CH_4 content.

At an equivalence ratio of 1.0, the primary inhibiting reaction shifts to R52, while R35 continues to exhibit significant inhibitory tendencies. Additionally, it's noticeable that the sensitivity coefficients of R38 and R52 undergo a much greater change with a decrease in CO_2 concentration compared to a decrease in N_2 concentration. This suggests that the impact of CO_2 on sensitivity is greater than that of N_2. At an equivalence ratio of 1.4, the increased sensitivity coefficients of R74 and R3 become more significant, while the impact of R35 in inhibiting reactions decreases, replaced by reaction R53, correlating with the relatively higher concentration of CH_4. Overall, with an increase in equivalence ratio, the absolute values of sensitivity coefficients for each elementary reaction also tend to increase.

3.4. Flame temperature and flame structure analysis

3.4.1 Flame temperature

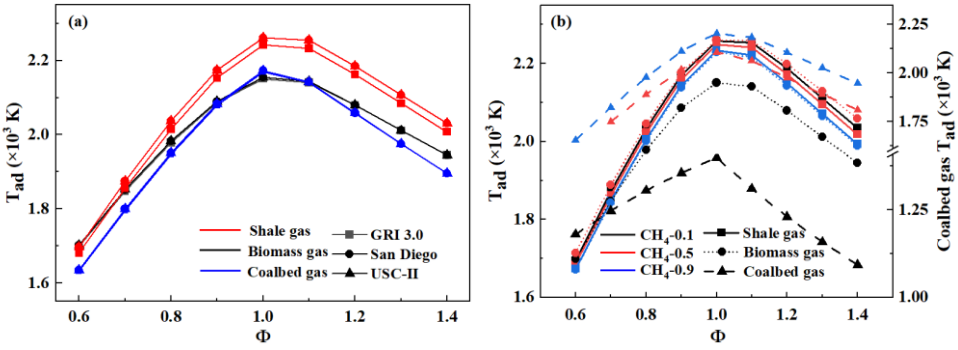

Fig. 8 Adiabatic flame temperature (T_{ad}) of different components (T_0 = 300 K, P_0 = 0.1 MPa)

Flame temperature, as a key characteristic of flame, plays a crucial role in the combustion process of fuel mixture. It is worth noting that flame temperature exhibits a positive correlation with the S_L of the fuel mixture [48].

Fig. 8(a) shows the curves of the variation of T_{ad} [49] with the equivalent ratio for the three gases calculated under different models. The simulation calculations of the three models are similar for the T_{ad}, so they can be effectively simulated. CH_4, C_2H_6, and C_3H_8 have similar T_{ad}. Influenced by dilute gases (CO_2 and N_2), the temperature of biomass gas and coalbed gas is lower than that of shale gas. Compared with coalbed gas, the temperature of biomass gas under lean and rich combustion

conditions is higher. In practice, it is almost impossible to reach the T_{ad}. Some of the heat of the flame is lost through thermal radiation and convection. However, the corresponding analysis can be effectively applied to calculate combustion efficiency and heat transfer processes. For high-temperature flame (above 1800K), the combustion products undergo a decomposition reaction, which not only increases the volume but also absorbs a lot of heat. At low temperatures, only CO_2 and H_2O should be produced after the combustion of a chemical equivalence ratio mixture or lean fuel mixture. However, these products are very unstable. As long as the temperature is slightly higher, they may be partially converted into simple molecular, atomic, and ionic forms (for example, CO, H_2, O, H, and OH). Accordingly, during the transformation process, the energy is absorbed and the maximum flame temperature is correspondingly reduced.

Fig. 8(b) shows three different CH_4 concentrations that are set, and the changes in T_{ad} are analyzed for each of the three gases at various equivalence ratios. For shale gas, as the proportion of CH_4 content gradually replaces the proportion of C_2H_6, the difference in T_{ad} is not significant. Combined with the above conclusions, it is determined that the T_{ad} is not the main reason for the increase in flame speed. When the content of dilute gas in the biomass gas is large, the content of dilute gas gradually decreases as the CH_4 content increases, which can effectively increase the flame temperature. As CH_4 gradually replaces the proportion of CO and H_2, the content of the two as high calorific value fuel the reduced content will reduce the T_{ad} to some extent. However, the combustion temperature is still better than the gas mixture with diluted gas. The change of coalbed gas is relatively simple. With the proportion of CH_4 replacing CO_2, it is evident from the picture that there is a huge increase in flame temperature. Relatively speaking, the temperature increase is greater than the proportion of CH_4 replacing N_2.

Fig. 9 shows the flame temperature sensitivity coefficients of three gases under stoichiometric conditions based on the GRI mechanism file. Fig. 9(a) is a comparison diagram of the temperature sensitivity coefficients of the three gases under basic data. For the three gases, R38($H + O_2 = O + OH$) and R52($H + CH_3 (+ M) = CH_4 (+ M)$) have the highest absolute value of sensitivity coefficients in the premixed zone. While the R99($OH + CO = H + CO_2$) of biomass gas becomes the highest and positive. Increasing the reaction rate will raise the flame temperature.

Fig. 9(b), (c) and (d) show the temperature sensitivity coefficients of shale gas, biomass gas, and coalbed gas under stoichiometric conditions under different CH_4 concentrations. Fig. 9(b) shows the temperature sensitivity coefficient of shale gas. Select five reactions that reflect the change in CH_4 content. In the pre-combustion zone, with the increase of CH_4 content, the absolute values of sensitivity coefficients of R52 and R38 increase. In the reaction zone, the reaction rates of the basic reactions R52 and R35($H + O_2 + H_2O = HO_2 + H_2O$), which promote the temperature rise, gradually decrease in the reaction zone, will inhibit the heating of the flame. In contrast, the elementary reaction R38 which inhibited flame temperature increased with the change in CH_4 concentration. The temperature sensitivity coefficient of biomass gas is shown in Fig. 9(c) according to the change curve of CH_4 concentration. In the pre-combustion zone, the negative and positive sensitivity coefficients of R38 and R52 are the largest, and the reaction moves forward to a certain extent with the increase of CH_4 concentration, while the absolute value of the sensitivity coefficient also increases. However, it is observed that R35 exhibits a higher value at 50% CH_4 content. Within the reaction zone, the peak of endothermic reaction R38 gradually shifts backwards and intensifies, resulting in a prolonged reaction duration and subsequent temperature decrease within the reaction zone.

The elementary reactions R52 and R35 that promote temperature rise are both decreasing. The rate of decline increases as the CH_4 content increases. Fig. 9(d) shows the temperature sensitivity coefficient of coalbed gas with CH_4 content. In the pre-combustion zone, as the proportion of CH_4 content increases, the absolute values of the sensitivity coefficients of reactions R38 and R52 decreased significantly in the initial phase, while the other reactions decreased slightly in the initial phase. but gradually increase with the transition to the reaction zone. Both R52 and R35, which promote the temperature increase in the reaction zone, showed a decreasing trend. However, with the increase of CH_4, the decrease rate slowed down, and the overall temperature in the reaction zone increased. By examining the characteristics of flame speed, it is determined that the flame speed and temperature of multi-component fuels exhibit independence from each other, with chemical action playing a more significant role than thermal action in the combustion process.

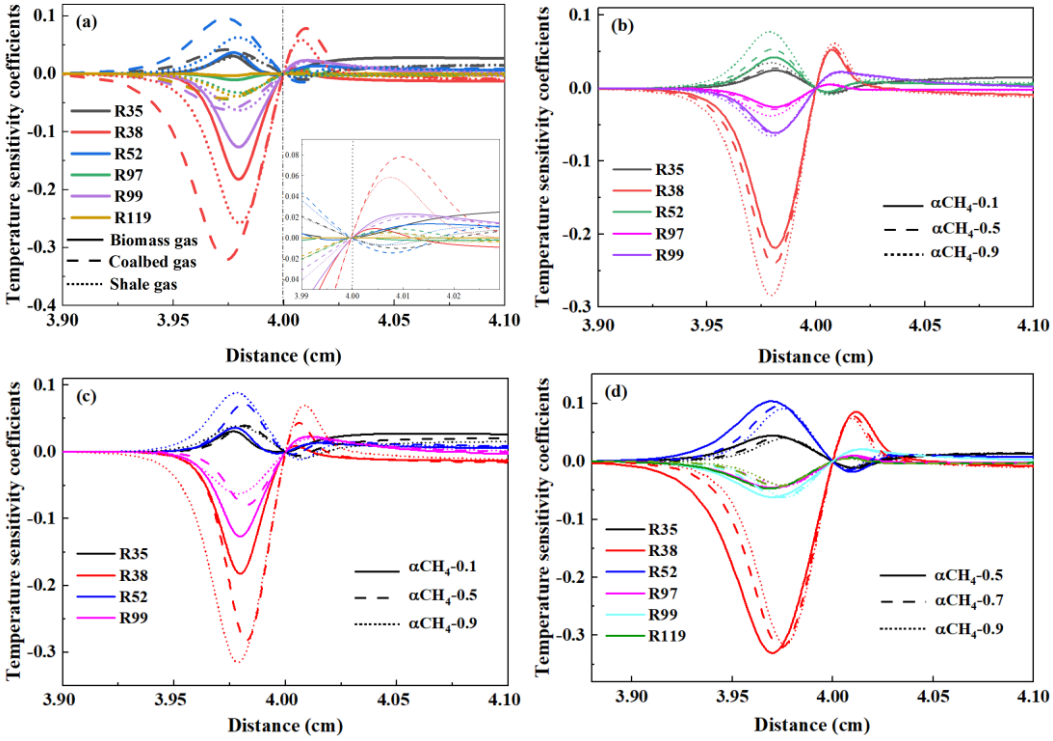

Fig. 9 Temperature sensitivity coefficients of three gases (T_0 = 300 K, P_0 = 0.1 MPa)

3.4.2 Flame structure analysis

The flame structure of three gas-premixed combustion flames can be analyzed by studying the changes in the concentration of various substances during flame propagation. Including the chemical reaction zone free radical concentration distribution curve, T_{ad} change curve, and reactant and product concentration change curve. Free radical-induced chain propagation and chain-induced reaction are the driving force of flame propagation. Free radical concentration plays a very important role in premixed laminar flow combustion and is important data to measure flame stability.

The mole fractions and temperature distribution characteristics of the main components of the three gases, calculated using the GRI 3.0 model under normal pressure and temperature conditions (T_0 = 300 K, P_0 = 0.1 MPa), are illustrated in Fig. 10. Fig. 10(a) shows the variation law of temperature degree distribution and mole fraction of main components in shale gas. Compared with CH_4, C_2H_6 with two carbon atoms need more oxygen for complete combustion. To maintain the equivalence ratio

of 1, less air will be involved. In addition, because the ratio of the number of hydrocarbon atoms in CH_4 is 1:4, compared with C_2H_6 with the number of hydrocarbon atoms of 1:3, the molar fraction of CO_2 produced by the combustion of CH_4 per unit of material will decrease, while the mole fraction of H_2O will increase. CO plays an irreplaceable role in the oxidation of hydrocarbons, and the combustion of hydrocarbon fuels can be simply divided into two steps: First, the fuel bond breaks to form CO, and the second step is the final oxidation of CO to CO_2. Among them, the basic reaction R99 is a chain transfer reaction that can effectively promote the combustion of hydrocarbon fuels. The mole fraction of CO decreases with increasing CH_4 concentration, which will slow down the forward progress of reaction R99, thus inhibiting the S_L, which is also consistent with the sensitivity coefficient analysis.

Fig. 10(b) shows the temperature distribution of biomass gas and the change of mole fraction of main components. The involvement of CH_4 in the chain termination reaction R52 leads to significant consumption of OH, H, and O radicals, resulting in a reduction in the overall chemical reaction rate. Consequently, there is a corresponding decrease in the flame speed of the fuel mixture. Additionally, with an increasing concentration of CH_4, the mole fraction of CO initially increases and then subsequently decreases. This is also due to the initial oxidation of hydrocarbon fuel to generate CO, which increases the mole fraction of CO. As CH_4 is about to be depleted, the mole fraction of CO begins to slowly decline because CO compete weakly on the O radical. CO is gradually oxidized when there is an excess of O radicals. In the presence of diluted gas, CH_4 is more susceptible to the temperature rise rate of the flame than hydrogen. The maximum heating rate occurs when the CH_4 is depleted and the CH_4 concentration is not the largest factor affecting the temperature. Therefore, the inhibitory effect of CH_4 on biomass gas flame speed is mainly the result of chemical and thermal effects.

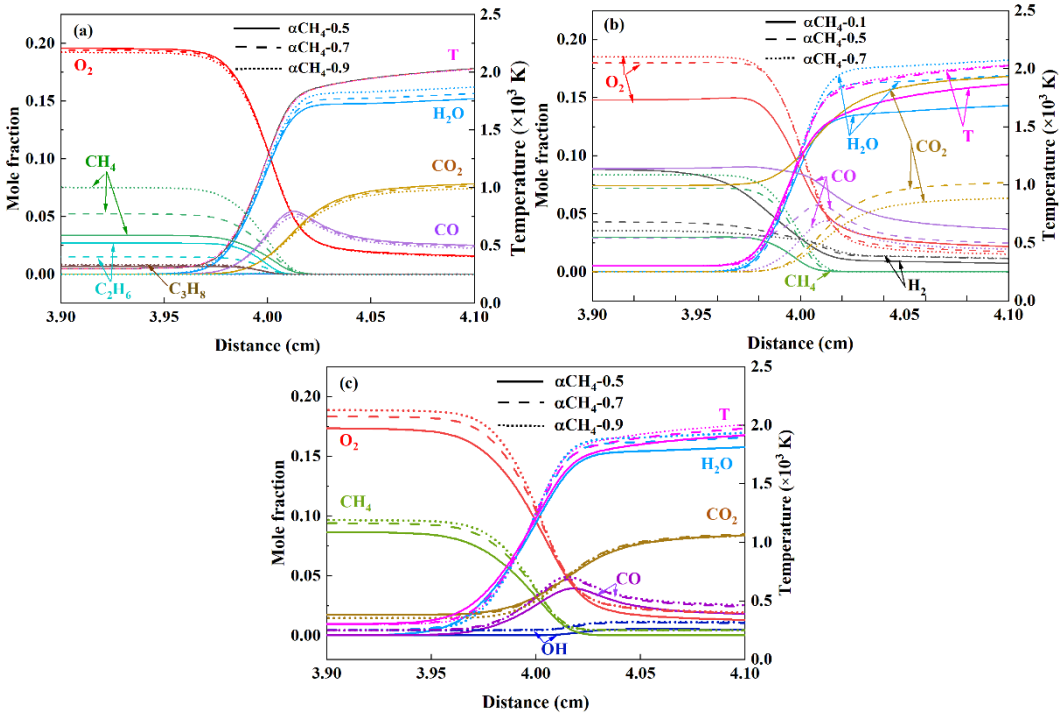

Fig. 10 Mole fractions and temperature distributions of the three gases (T_0 = 300 K, P_0 = 0.1 MPa)

In Fig. 10(c), the mole fraction of CO also initially increases as the reaction progresses and slowly decreases when CH_4 is about to be consumed completely. With an increase in CH_4 content, the required amount of O_2 for the reaction also increases. When the CH_4 content increases from 50% to 70%, the molar fraction of CO will significantly increase, whereas an increase from 70% to 90% CH_4 content will result in only a small increase in the molar fraction of CO.

4. Conclusion and analysis

1. In shale gas, CH_4 has an inhibitory effect on the S_L of the mixture. The inhibitory effect decreases first and then increases as the equivalence ratio increases. In biomass gas, as CH_4 replaces CO, the S_L gradually decreases, and the rate of decrease is faster with higher equivalence ratios. In coalbed gas, as the CH_4 content increases, the S_L increases, and CO_2 has a stronger inhibitory effect on the S_L.

2. In shale gas and biomass gas, the physical effect resulting from the addition of CH_4 is greater than the chemical effect produced by CH_4, and as the CH_4 content increases, the ratio of chemical effect to physical effect decreases, leading to a reduction in the S_L of the mixed fuel. In coalbed gas, due to the thermal and chemical effects of CO_2, CO_2 exhibits a greater inhibitory effect on the fuel compared to an equal volume fraction of N_2.

3. In shale gas, the forward reaction R38 and the inhibitory reaction R52 exhibit the highest sensitivity coefficients, which increase with the CH_4 content. In biomass gas, the forward and inhibitory reactions with the greatest sensitivity coefficients remain to be R38 and R52, however, the sensitivity coefficients increase with a decrease in CO content and decrease with a reduction in H_2 content. In coalbed gas, the forward reaction R38 shows the highest positive sensitivity coefficient, while the reaction with the highest negative sensitivity coefficient in the lean burn region is R35, which gradually transitions to R52 with an increase in equivalence ratio.

4. In shale gas, the consumption of CH_4 and C_2H_6 progressions approximately simultaneously, while the molar fraction of CO initially increases and then decreases as the reaction proceeds, playing a significant role in the reaction. In biomass gas, in the presence of diluting gases, CH_4 is more susceptible to the flame heating rate compared to H_2. The maximum heating rate occurs when CH_4 is depleted. In coalbed gas, the molar fraction of CO initially rises and then falls as the reaction progresses, starting to decrease as CH_4 is about to be consumed completely.

Acknowledgment

The authors appreciate the support of the Key Science and Technology Program of Henan Province, 232102321082, 232102221017.

References

[1] Le Minh Thong, Tung DH, Thuy NT, et al. What prospects for shale gas in Asia? Case of shale gas in China. The Journal of World Energy Law & Business. 2021; 13:426-40.

[2] Dong X, Peng L, Xiaoyou Y, et al. Energy consumption and greenhouse gas emissions of shale gas chemical looping reforming process integrated with coal gasification for methanol production. APPL THERM ENG. 2021; 193.

[3] Liu D, Wang H, Zhao Q, et al. Major Understanding and Innovation, Challenges and Potential

analysis of Shale Gas Exploration and Development in China., 2020 International Conference on New Energy,Power and Environmental Engineering(NEPEE2020)2020.p.5.
[4] School Of Mechanical Engineering SJUC, School Of Mechanical Engineering SJUC. A review on mixing laws of laminar flame speed and their applications on H_2/CH_4/CO/air mixtures. INT J HYDROGEN ENERG. 2020; 45:20482-90.
[5] Matamba T, Tahmasebi A, Yu J, et al. A review on biomass as a substitute energy source: Polygeneration influence and hydrogen rich gas formation via pyrolysis. J ANAL APPL PYROL. 2023; 175:106221.
[6] Yao D, Xu Z, Qi H, et al. Carbon footprint and water footprint analysis of generating synthetic natural gas from biomass. RENEW ENERG. 2022; 186:780-9.
[7] Prasun B, Ranjan P, Kumar SR, et al. Investigation on Barail Formation Coals of Upper Assam with Reference of Coal Bed Methane (CBM). J GEOL SOC INDIA. 2023; 99:99-104.
[8] Dev J, Piyush P, Pushpa S, et al. Past, present and future of Coal Bed Methane (CBM): a review with special focus on the Indian scenario. INT J COAL PREP UTIL. 2023; 43:377-402.
[9] Jianchao H, Zhiwei W, Pingkuo L. Current states of coalbed methane and its sustainability perspectives in China. INT J ENERG RES. 2018; 42:3454-76.
[10] Vargas AC, Arrieta AA, Arrieta CE. Combustion characteristics of several typical shale gas mixtures. J NAT GAS SCI ENG. 2016; 33:296-304.
[11] Ozturk S. A Numerical Investigation on Emissions of Partially Premixed Shale Gas Combustion. INT J HEAT TECHNOL. 2020; 38:745-51.
[12] Bhasker JP, Porpatham E. Effects of compression ratio and hydrogen addition on lean combustion characteristics and emission formation in a Compressed Natural Gas fuelled spark ignition engine. FUEL. 2017; 208:260-70.
[13] Miao H, Liu Y. Measuring the laminar burning velocity and Markstein length of premixed methane/nitrogen/air mixtures with the consideration of nonlinear stretch effects. FUEL. 2014; 121:208-15.
[14] Zheng S, Zhang X, Wang T, et al. An experimental study on premixed laminar and turbulent combustion of synthesized coalbed methane. ENERGY. 2015; 92:355-64.
[15] Mahdi SH, Al-Dulaimi ZM. Flame Speed and Laminar Burning Velocity in Syngas/Air Mixtures: A Review. Instrumentation Mesure Métrologie. 2022; 21.
[16] Abdulameer AA, Mahmood SA, AK SH. Measurements and Data Analysis Review of Laminar Burning Velocity and Flame Speed for Biofuel/Air Mixtures. IOP Conference Series: Materials Science and Engineering. 2021; 1094:12029.
[17] E SI, S WA, G UDF, et al. Flame characteristics analysis of a methane gas' premixed combustion on a ring attached-bunsen burner using ansys fluent. Journal of Physics: Conference Series. 2022; 2193.
[18] Rushikesh K, Shreya P, Valentina V, et al. CFD approach to predict the significance of the shape bluff body on flame stabilisation in lean premixed combustion of hydrogen-air mixtures. Materials Today: Proceedings. 2023; 72:1181-9.
[19] Yanfei Z, Dapeng Z, Qin L, et al. Premixed combustion and emission characteristics of methane diluted with ammonia under F-class gas turbine relevant operating condition. FRONT ENERGY RES. 2023.
[20] Tingquan T, Chengbin S, Haiou W, et al. The effects of turbulence on the flame structure and

NO formation of ammonia turbulent premixed combustion at various equivalence ratios. FUEL. 2023; 332.
[21] Liu Z, He X, Jiang Z, et al. Study on the laminar combustion characteristics and kinetic of IC_8H_{18}/NH_3 premixed flames. FUEL. 2024; 356:129633.
[22] Oppong F, Luo Z, Li X, et al. Laminar combustion characteristics of ethyl acetate/hydrogen/air at elevated pressures. FUEL. 2022; 330:125631.
[23] Pessina V, Berni F, Fontanesi S, et al. Laminar flame speed correlations of ammonia/hydrogen mixtures at high pressure and temperature for combustion modeling applications. INT J HYDROGEN ENERG. 2022; 47:25780-94.
[24] Dong W, Jin T, Qiu B, et al. Effects of carbon dioxide on the combustion characteristics of the laminar premixed n-heptane/air flames at elevated pressures. J ENERGY INST. 2021; 99:127-36.
[25] Gregory P. Smith DMGM. http://www.me.berkeley.edu/gri_mech/.
[26] Hai Wang X. USC Mech Version II. High-Temperature Combustion Reaction Model of H_2/CO/C1-C4 Compounds. http://ignis.usc.edu/USC_Mech_II.htm. 2007..
[27] Chemical-Kinetic Mechanisms for Combustion Applications, San Diego Mechanism web page, Mechanical and Aerospace Engineering (Combustion Research), University of California at San Diego (http://combustion.ucsd.edu)..
[28] VinaySankar, V J, AkramMohammad, et al. Effect of Hydrogen Addition on Laminar Burning Velocity of Liquefied Petroleum Gas Blends. ENERG FUEL. 2019; 34:798-805.
[29] Guoyan C, Shuangshuang Z, Junsheng Z, et al. Experimental and numerical simulation of effects of CO_2/N_2 concentration and initial temperature on combustion characteristics of biomass syngas. J SAUDI CHEM SOC. 2022; 26.
[30] Zhou S, Zhu X, Li B, et al. Experimental and numerical study on adiabatic laminar burning velocity and overall activation energy of biomass gasified gas. FUEL. 2022; 320:123976.
[31] Maria M, Codina M, Venera G. The Laminar Burning Velocities of Stoichiometric Methane–Air Mixture from Closed Vessels Measurements. ENERGIES. 2022; 15:5058.
[32] Wang Q, Song Y, Liu K, et al. Laminar combustion characteristics of methane/methanol/air mixtures: Experimental and kinetic investigations. CASE STUD THERM ENG. 2023; 41:102593.
[33] Zhai Y, Wang S, Wang Z, et al. Experimental and numerical study on laminar combustion characteristics of by-product hydrogen coke oven gas. ENERGY. 2023; 278:127766.
[34] Cardona Vargas A, Amell Arrieta A, Arrieta CE. Combustion characteristics of several typical shale gas mixtures. J NAT GAS SCI ENG. 2016; 33:296-304.
[35] Etiope G, Drobniak A, Schimmelmann A. Natural seepage of shale gas and the origin of “eternal flames” in the Northern Appalachian Basin, USA. MAR PETROL GEOL. 2013; 43:178-86.
[36] William L, de Vries Jaap, Michael K, et al. Laminar Flame Speed Measurements and Modeling of Pure Alkanes and Alkane Blends at Elevated Pressures. Journal of Engineering for Gas Turbines and Power. 2011; 133.
[37] Zhang Y, Liang Y, Li S, et al. A review of biomass pyrolysis gas: Forming mechanisms, influencing parameters, and product application upgrades. FUEL. 2023; 347:128461.
[38] Song W, Chen X, Huang Y, et al. Thermal analysis technology to utilize waste biomass and waste heat to produce high-quality combustible gas through simulations and experiments. SCI TOTAL ENVIRON. 2023; 892:163970.
[39] Yao D, Xu Z, Qi H, et al. Carbon footprint and water footprint analysis of generating synthetic

natural gas from biomass. RENEW ENERG. 2022; 186:780-9.
[40] Chen X, Wang Y, Tao M, et al. Tracing the origin and formation mechanisms of coalbed gas from the Fuxin Basin in China using geochemical and isotopic signatures of the gas and coproduced water. INT J COAL GEOL. 2023; 267:104185.
[41] Tu Z, Li L, Wang F, et al. Review on separation of coalbed methane by hydrate method. FUEL. 2024; 358:130224.
[42] Wang Y, Fan X, Niu K, et al. Estimation of hydrogen release and conversion in coal-bed methane from roof extraction in mine goaf. INT J HYDROGEN ENERG. 2019; 44:15997-6003.
[43] Zhang Q, Chen G, Wang F, et al. Experimental and model analyses of laminar combustion characteristics of variable composition $CO/H_2/CH_4$ mixtures at high N_2 and CO_2 concentrations. INT J ENERG RES. 2020; 44:7507-24.
[44] Chen J, Chen G, Zhang A, et al. Experimental and numerical study on the effect of CO_2 dilution on the laminar combustion characteristics of premixed CH_4/H_2/air flame. J ENERGY INST. 2022; 102:315-26.
[45] Ge Y, Ma H, Wang L. Experimental and numerical investigation of combustion characteristics of carbon-free NH_3/H_2 blends in N_2O. INT J HYDROGEN ENERG. 2024; 49:510-20.
[46] Oppong F, Zhongyang L, Li X, et al. Methyl pentanoate laminar burning characteristics: Experimental and numerical analysis. RENEW ENERG. 2022; 197:228-36.
[47] Li H, Xiao H. Effect of H_2 addition on laminar burning velocity of NH_3/DME blends by experimental and numerical method using a reduced mechanism. COMBUST FLAME. 2023; 257:113000.
[48] Law CK. Combustion Physics. Cambridge University Press, 2010.
[49] Xiang L, Chu H, Ren F, et al. Numerical analysis of the effect of CO_2 on combustion characteristics of laminar premixed methane/air flames. J ENERGY INST. 2019; 92:1487-501.

Submitted: 14.01.2024.
Revised: 25.03.2024.
Accepted: 28.03.2024.